

## Supporting Information

# Preparation, characterization, and bio-degradation studies of high-performance bio-based polyimides based on bicyclic diamines derived from citric acid

Xueshuang Jiang, Yubo Long, Kaijin Chen, Qiaoxi Yu, Zhenguo Chi, Siwei Liu\*, Jiarui Xu, and Yi Zhang\*

## 1. Detailed experimental procedure

### 1.1. Synthesis of the polyimide films

Biomass-based polyimides were prepared by two different methods, chemical and thermal imidization. The reaction schemes are shown in Scheme 2. Equimolar amounts of dianhydride and diamine monomers were used in all cases. Typically, for PI(FAC), OAC (0.82 g, 0.002 mol) and 6FDA (0.888 g, 0.002 mol) were transferred to a 50 mL three neck flask equipped with mechanical stirring under nitrogen, and then DMAc (9.98 mL) was added to make the solids content at 15%. The resulting mixture was continuously stirred for 18 h at room temperature to obtain viscous PAA solution.

In this work, chemical imidization was conducted by gradually adding a mixed solution of Ac<sub>2</sub>O/pyridine (7/3, v/v) to PAA solutions (solid content: 10-20 wt%) at a feeding molar ratio of [Ac<sub>2</sub>O]/[COOH]<sub>PAA</sub> = 5 with continuously vigorous stirring at room temperature. The reaction mixture was then stirred at room temperature for 24 h in a sealed flask. The homogeneous solution was adequately diluted with the same solvent, and was slowly poured into a large quantity of ethanol. Then the obtained fibrous precipitate was repeatedly washed with fresh ethanol, collected by filtration, and dried at 60 °C in vacuum for 12 h. The dried PIs fiber was dissolved in fresh DMAc at 10-20 wt%. Subsequently, the homogeneous PIs solution was coated on a glass substrate and dried at 60 °C for 1 h in an air-convection oven and followed by the heat imidization of PI solution cast onto a flat glass plate under a gradient heating temperature (80 °C for 1 h, 180 °C for 1 h, 250 °C for 1 h) in vacuum oven. After peeling them off the substrate, the PIs films (typically 20-30 μm thick) were successively annealed in vacuum at temperatures 10-20 °C lower than the *T<sub>g</sub>*'s to eliminate residual stress in the film samples while avoiding undesirable significant film deformation.

## 2. Details of measuring method

### 2.1. General methods

All Nuclear Magnetic Resonance spectra (NMR) were recorded on a Bruker AVANCE 400 spectrometer. Samples were prepared as solution of 5~15 mg of compound in 0.5 mL of deuterated dimethyl sulfoxide (DMSO) using tetramethylsilane (TMS) as the internal reference. Mass spectra were recorded on Thermo EI mass spectrometer (DSQ II) and Matrix-assisted laser desorption ionization time-of-flight mass spectrometry (MALDI-TOF-MS, REFLEX III). Elemental analysis was conducted with CHNS elemental analyzer. Infrared spectra (IR) were obtained by using a BRUKER TENSOR 27 Fourier-transform infrared (FT-IR) spectrometer. Absorption spectra were measured by a Hitachi UV-Vis spectrophotometer (U-3900) in the range of 200-800 nm. The intrinsic viscosity ( $\eta$ ) of polyimides were measured at a solid content of 0.5 wt% in DMF at 30 °C on an Ostwald viscometer. Optical rotation is measured by a SCHMIDT + HAENSCH POLARTRONIC HHW5 polarimeter at 25 °C using DMAc as solvent. Wide-angle X-ray diffraction (WAXD) was measured on a Rigaku Smart Lab X-ray diffractometer. Thermogravimetric analyses (TGA) were performed with a TG209F1 libra thermal analyzer under N<sub>2</sub> with a heating rate of 10 °C·min<sup>-1</sup> from 50 to 800 °C, and heated under flowing nitrogen (20 mL·min<sup>-1</sup>). The dynamic mechanical (DMA) spectra of the samples were obtained by using DMA Q800 analyzer. The specimens were analyzed in tensile mode at a constant frequency of 1 Hz, tensile mode at a preload force of 0.01 N, and a temperature range from 50 to 325 °C at a heating rate of 10 °C·min<sup>-1</sup>. Thermal mechanical analysis (TMA) was used to study the coefficient of thermal expansion of the film with a heating rate of 10 °C·min<sup>-1</sup> from 50 °C to 320 °C by TMA Q400 instrument under nitrogen. Tensile test was performed on samples cut from 35~50 μm thick sheet and tested using SANS CMT6103 instrument according to GB/T16421-1996. The specimen size is 10 × 100 mm, Jaw separation is 50 mm. Jaw speed was first set to 2 mm·min<sup>-1</sup>. Results were carried out with three film specimens. The morphology of the surface of PI films was measured by a Hitachi S-4800 field emission scanning electron microscope (SEM) and the samples were sputter-coated with 100 Å of gold before scanning.

### 2.2. Biodegradation and hydrolytic degradation

Films for polyimide biodegradation and hydrolytic degradation studies were prepared with a thickness of 20 ± 5 μm. The films were cut into 10 mm diameter, 3-4 mg weight disks and dried in vacuum to constant weight. For hydrolytic degradation, samples were immersed in vials containing 10 mL of either citric acid buffer (pH 2.0) or sodium phosphate buffer (pH 7.4) at 37 °C. After incubation for the scheduled period

of time, the samples were rinsed thoroughly with distilled water and dried to constant weight. The enzymatic degradation was carried out at 37 °C in vials containing 10 mL of the enzymatic medium, consisting of a pH 7.4 buffered sodium phosphate solution containing lipase from porcine pancreas (10 mg). The buffered enzyme solution was replaced every 72 h to maintain the enzyme activity. At the end of the scheduled incubation periods, the disks were withdrawn from the incubation medium, washed thoroughly with distilled water, dried to constant weight and analyzed by GPC chromatography, NMR spectroscopy and SEM microscopy.

### 2.3. Construction of polymer microstructures

Biovia Materials Studio software was employed to perform simulations in this study using the COMPASS (Condensed-phase Optimized Molecular Potentials for Atomistic Simulation Studies) forcefield.<sup>1, 2</sup> Initially, polymer chains containing 25 repeat units were built and geometry optimization was performed. Based on the equilibrated models, the free volumes, radial distribution functions (RDFs), radius of gyration ( $R_g$ ) and movement capacity of chains were investigated. The construction of the model, simulation processes, and descriptions of properties can be found in the reported literature.<sup>3</sup>

## 3. Characterization

Nuclear Magnetic Data:

ONC: <sup>1</sup>H NMR (400 MHz, DMSO-*d*<sub>6</sub>),  $\delta$  (ppm): 10.30 (*s*, 2H, NH), 8.23 – 8.16 (*m*, 4H, Ph-H), 7.74 – 7.67 (*m*, 4H, Ph-H), 5.00 (*p*, *J* = 6.6, 2H, CH), 2.47 (*s*, 2H, CH), 2.25 (*ddd*, *J* = 13.5, 7.9, 5.8, 4H, CH<sub>2</sub>), 1.69 (*dt*, *J* = 12.9, 6.3, 4H, CH<sub>2</sub>). MS (APCI) *m/z*: [M + H]<sup>+</sup> calcd for C<sub>22</sub>H<sub>22</sub>N<sub>4</sub>O<sub>8</sub>, 470.44; found, 470.

OND: <sup>1</sup>H NMR (400 MHz, DMSO-*d*<sub>6</sub>),  $\delta$  (ppm): 8.23 – 8.13 (*m*, 4H, Ph-H), 7.16 – 7.06 (*m*, 4H, Ph-H), 4.94 (*p*, *J* = 5.9, 2H, CH), 2.64 – 2.52 (*m*, 2H, CH), 2.35 – 2.20 (*m*, 4H, CH<sub>2</sub>), 1.73 (*dt*, *J* = 13.2, 5.6, 4H, CH<sub>2</sub>). MS (APCI) *m/z*: [M + H]<sup>+</sup> calcd for C<sub>20</sub>H<sub>20</sub>N<sub>2</sub>O<sub>6</sub>, 384.13; found, 384.

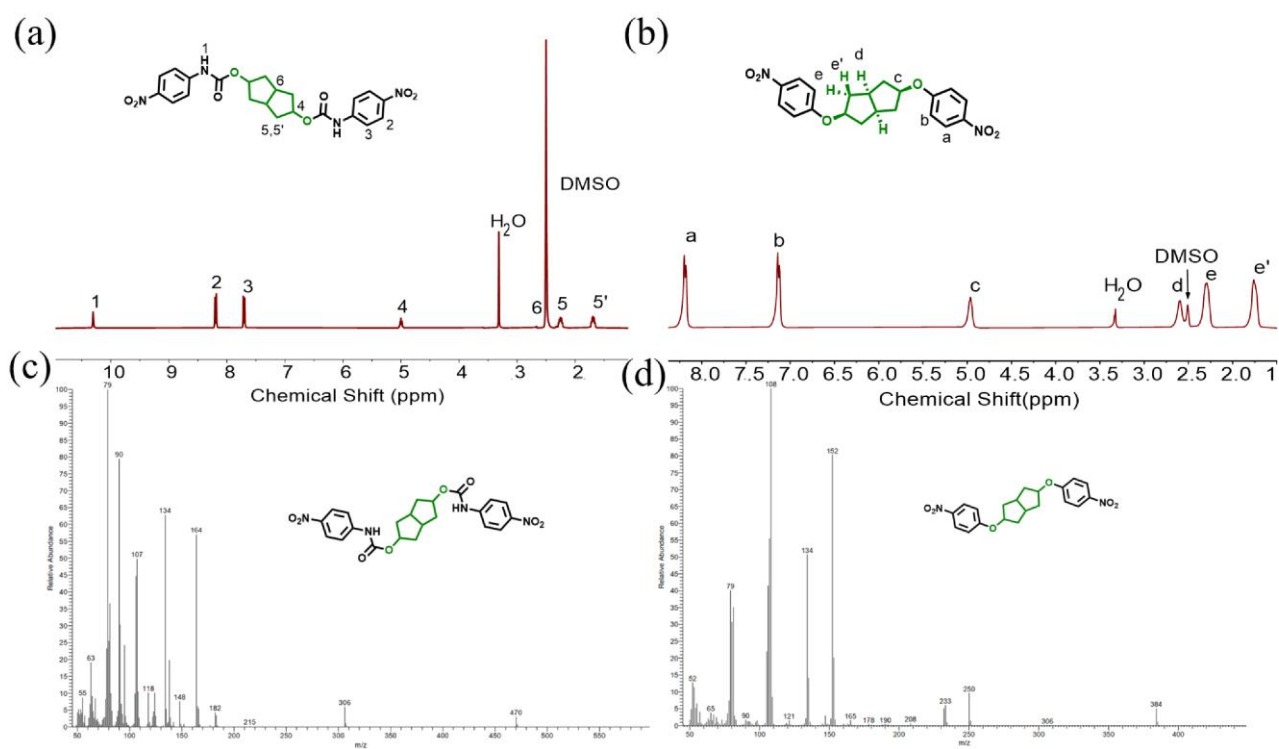


**Fig. S1** (a) and (b) <sup>1</sup>H-NMR spectra of ONC and OND. (c) and (d) EI-MS of ONC and OND.

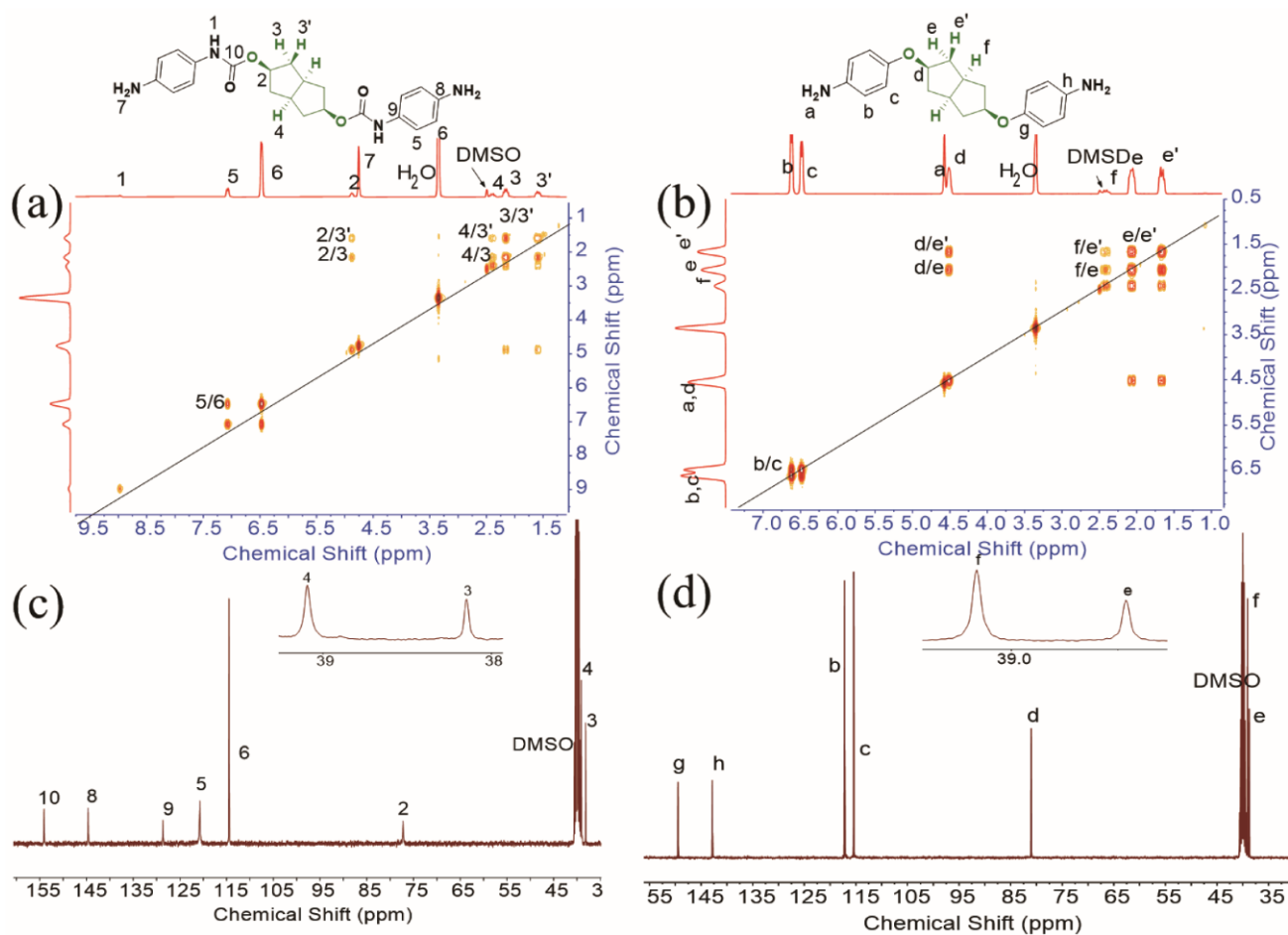


**Fig. S2** (a) and (b) 2D COSY spectrum of OAC and OOD recorded in DMSO, respectively. (c) and (d)  $^{13}\text{C}$  NMR spectrum of OAC and OOD recorded in DMSO, respectively.

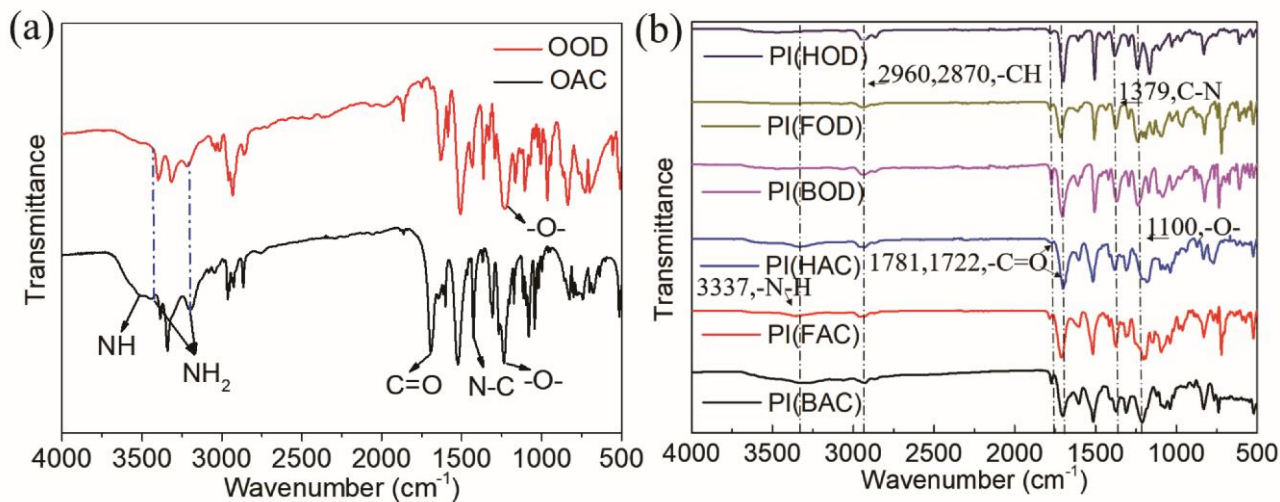


**Fig. S3** ATR-FTIR spectra of biomass-based (a) diamines and (b) polyimides films.

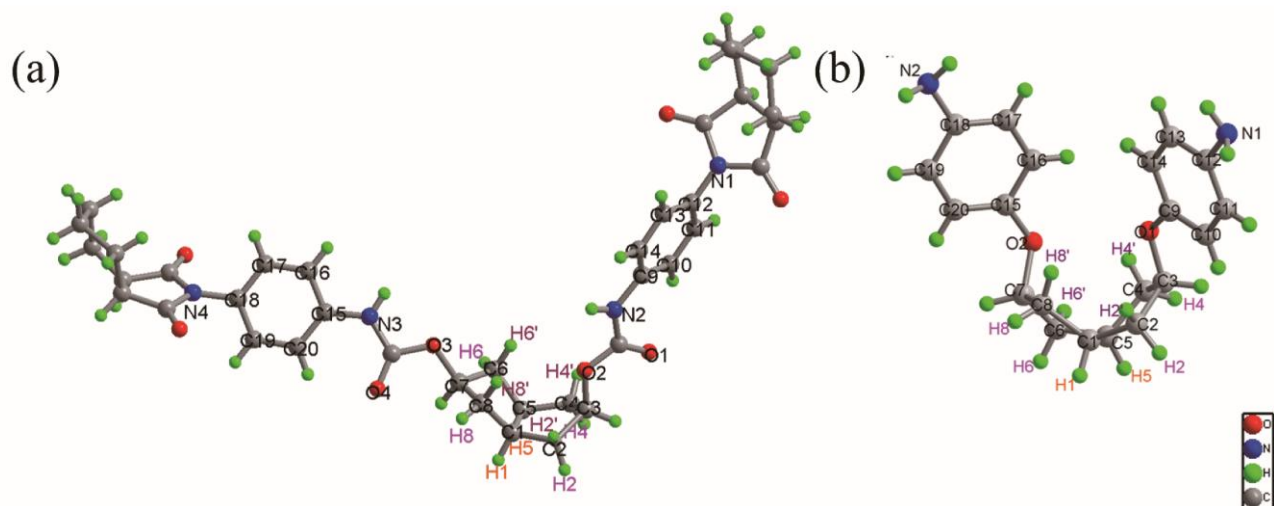


Fig. S4 Molecular structure of OAC-HDA and OOD in the crystal.

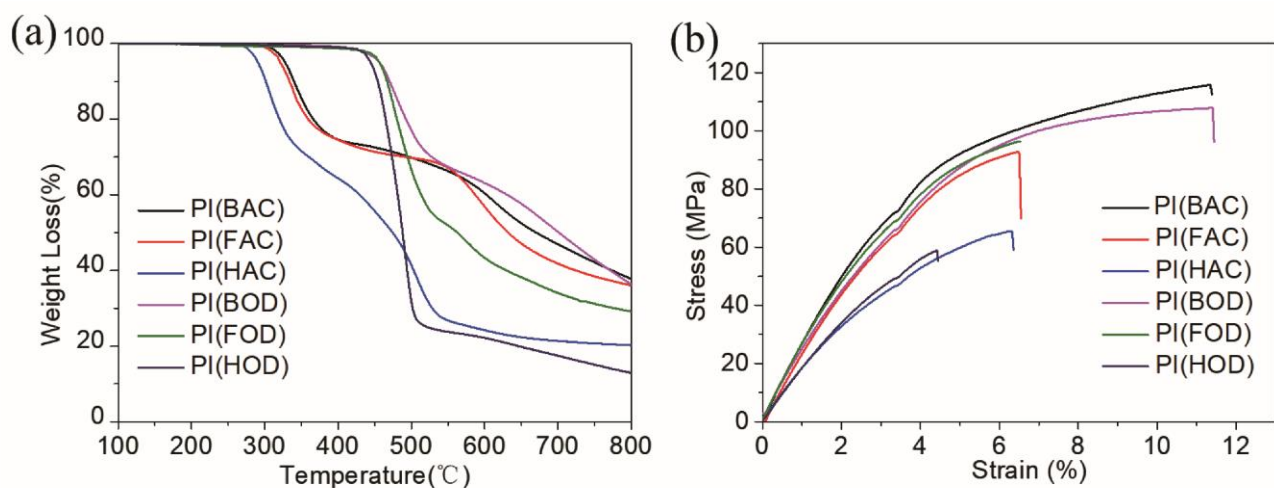


Fig. S5 (a) TGA curves of OAC-PIs and OOD-PIs at a heating rate of  $10\text{ }^{\circ}\text{C}\cdot\text{min}^{-1}$  under nitrogen atmosphere. (b) Stress-strain curves of OAC-PIs and OOD-PIs.

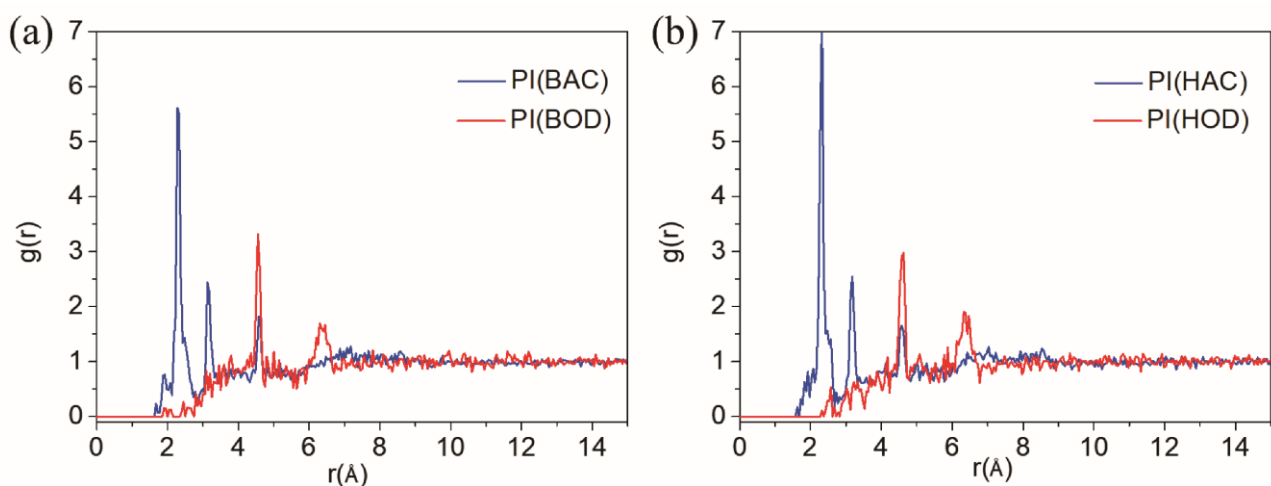


Fig. S6 Radial distribution function of (a) PI(BAC) and PI(BOD) and (b) PI(HAC) and PI(HOD) for the hydrogen atoms of  $\text{-HN-}$  and oxygen atoms of  $\text{O=C-}$  in carbamic acid ester and imide rings.

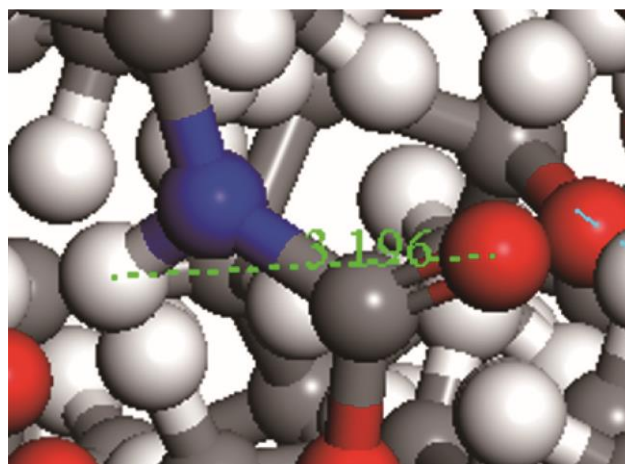


Fig. S7 The intramolecular hydrogen bond of carbamic ester.

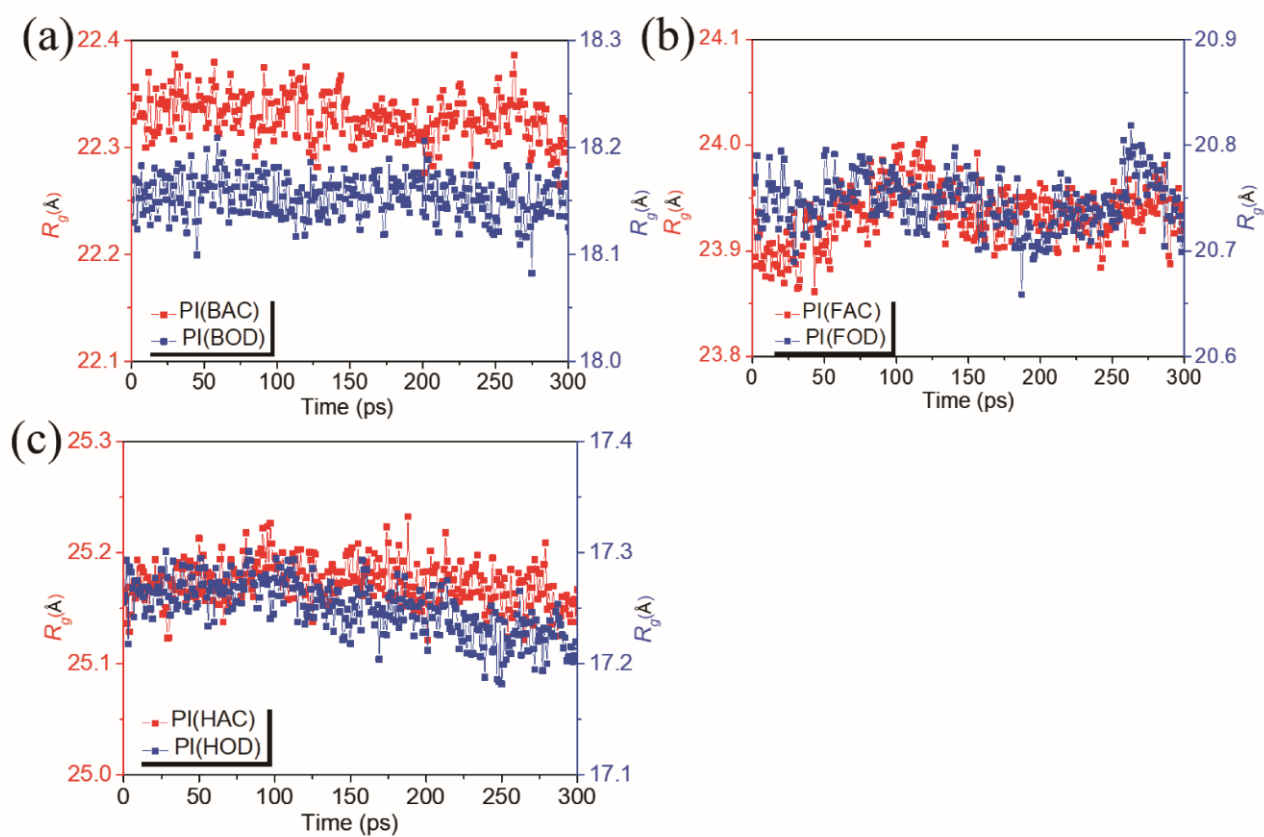
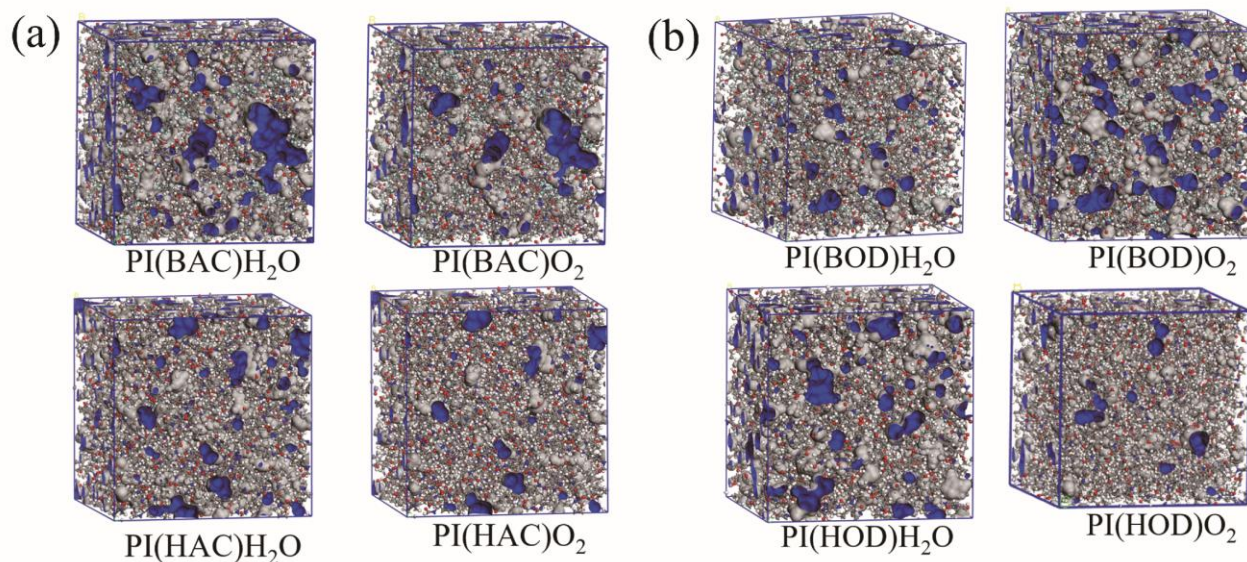
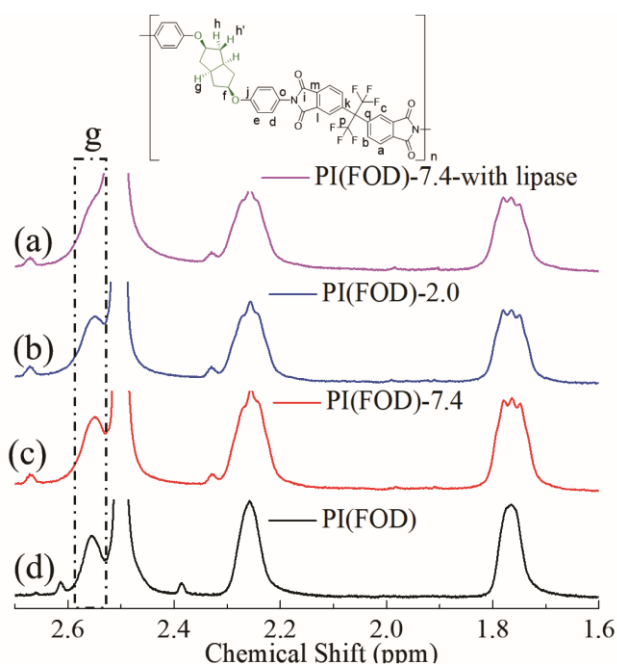


Fig. S8 Time dependence of the radius of gyration  $R_g$  for (a) PI(BAC) and PI(BOD). (b) PI(FAC) and PI(FOD) and (c) PI(HAC) and PI(HOD).



**Fig. S9** (a) PI(BAC) and PI(HAC) and (b) PI(BOD) and PI(HOD): H<sub>2</sub>O (a probe radius of 1.325 Å) and O<sub>2</sub> (a probe radius of 1.73 Å) accessible volumes for OAC-PIs (gray: van der Waals surface; blue: Connolly surface).



**Fig. S10** Compared <sup>1</sup>H NMR spectra in DMSO of PI(FOD) after incubation at pH 2.0 for 49 days (b); pH 7.4 with (a) and without (c) porcine pancreatic lipase for 49 days; initial sample (d).

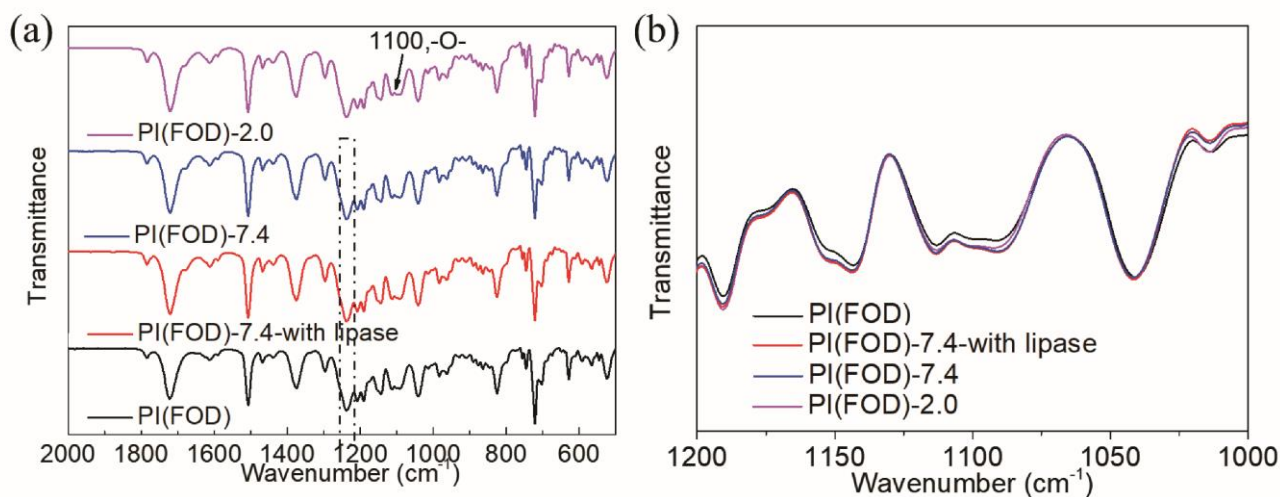


**Fig. S11** (a) ATR-FTIR spectra before and after incubation of PI(FOD). (b) An enlarged view of 1100  $\text{nm}^{-1}$  in Fig. 11a.

**Table S1.** Crystal data and structure refinement for OAC-HDA and OOD.

Identification code	OAC-HDA	OOD
Empirical formula	$\text{C}_{38}\text{H}_{42}\text{N}_2\text{O}_8$	$\text{C}_{20}\text{H}_{24}\text{N}_2\text{O}_2$
Formula weight	682.30	324.41
Temperature/K	149.99(10)	293(2)
Crystal system	orthorhombic	orthorhombic
Space group	$\text{P}2_12_12_1$	$\text{P}2_1$
$a/\text{\AA}$	10.39007(11)	7.6712(2)
$b/\text{\AA}$	10.69791(14)	11.1903(3)
$c/\text{\AA}$	30.6594(3)	19.6368(5)
$\alpha/^\circ$	90	90
$\beta/^\circ$	90	90
$\gamma/^\circ$	90	90
Volume/ $\text{\AA}^3$	3407.85(7)	1685.68(8)
Z	4	4
$\rho_{\text{calc}}/\text{cm}^3$	1.331	1.278
$\mu/\text{mm}^{-1}$	0.771	0.657
F(000)	1448.0	696.0
Crystal size/ $\text{mm}^3$	0.18/0.15/0.1	0.12/0.08/0.03
Radiation	$\text{CuK}\alpha$ ( $\lambda = 1.54184$ )	$\text{CuK}\alpha$ ( $\lambda = 1.54184$ )
$2\Theta$ range for data collection/ $^\circ$	5.766 to 145.054	8.908 to 145.248
Index ranges	$-12 \leq h \leq 7, -12 \leq k \leq 12, -25 \leq l \leq 37$	$9 \leq h \leq 9, -11 \leq k \leq 13, -23 \leq l \leq 22$
Data/restraints/parameters	6592/0/451	3279/0/219
Goodness-of-fit on $F^2$	1.035	1.040
Final R indexes [ $I \geq 2\sigma(I)$ ]	$R_1 = 0.0389, wR_2 = 0.1088$	$R_1 = 0.0366, wR_2 = 0.0957$
Final R indexes [all data]	$R_1 = 0.0400, wR_2 = 0.1101$	$R_1 = 0.0399, wR_2 = 0.0929$
Largest diff. peak/hole / $e \text{\AA}^{-3}$	0.48/-0.22	0.409/-0.172

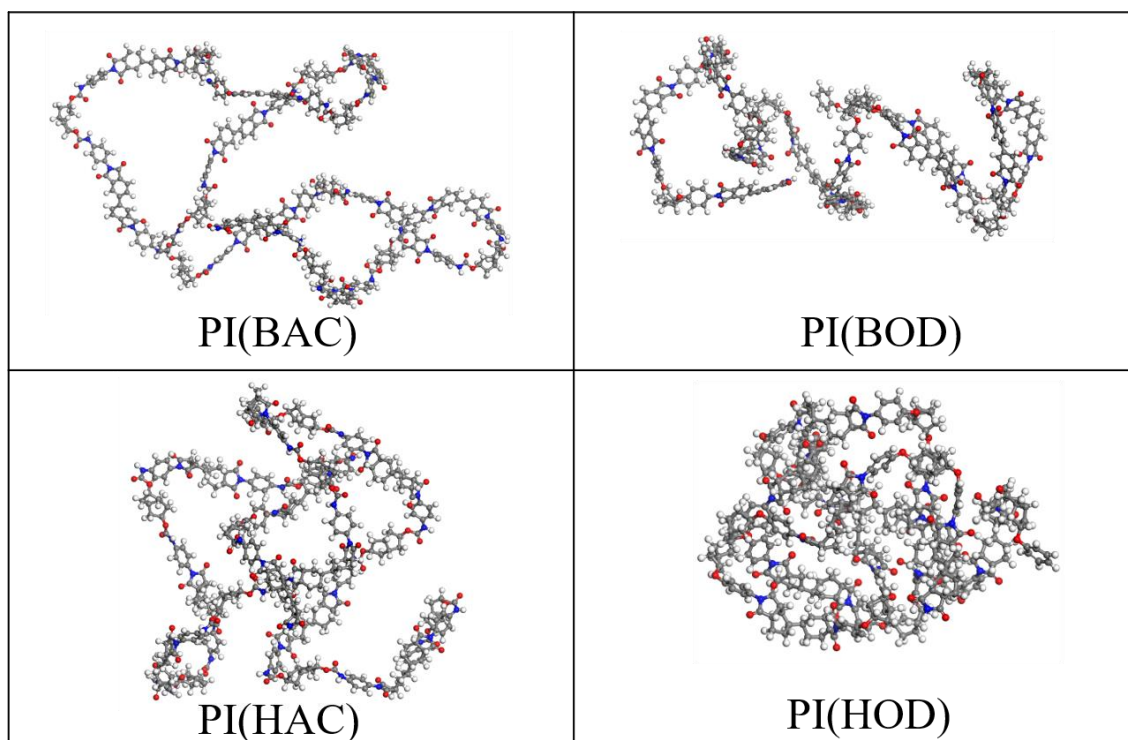
**Table S2.** The optical transmission date of OAC-PIs and OOD-PIs.

Polyimide	$T_{400}$ (%)	$\lambda_0$ (nm)	Total Optical Transmittance (%)
PI(BAC)	2	392	73.2
PI(FAC)	1.4	382	74.4
PI(HAC)	83.5	286	87.6
PI(BOD)	1	411	66.6
PI(FOD)	1	421	71.1
PI(HOD)	84.3	292	88.5

**Table S3.** Optical rotation of bio-based diamines and polyimides<sup>a</sup>.

Sample	OAC	PI(BAC)	PI(FAC)	PI(HAC)	OOD	PI(BAC)	PI(FAC)	PI(HAC)
$\alpha$ (°)	-0.0033	-	-0.0057	-0.0100	-0.0030	-	-0.0088	-0.0100
$[\alpha]_D$ (°cm <sup>3</sup> ·dm <sup>-1</sup> ·g <sup>-1</sup> )	-6.53	-	-11.45	-20.25	-6.00	-	-17.50	-20.10

<sup>a</sup>Measured at a concentration of 0.5 mg·ml<sup>-1</sup> in DMAc at 25 °C.

**Table S4.** Stereo view of the lowest energy conformations of the OAC-PIs and OOD-PIs.

## References

1. H. Sun, P. Ren and J. R. Fried, *Computational and Theoretical Polymer Science* 1998, **8**, 229-246.
2. H. Sun, *Journal of Physical Chemistry B*, 1998, **102**, 7338-7364.
3. Y. Liu, A. Tang, J. Tan, C. Chen, D. Wu and H. Zhang, *ACS Omega*, 2021, **6**, 4273-4281.